Proceedings of 20th International Congress on Acoustics, ICA 2010

23-27 August 2010, Sydney, Australia

Acoustic properties of hollow brick walls

Gary Jacqus (1,2), Sylvain Berger (1), Vincent Gibiat (2), Philippe Jean (3), Michel Villot (3) & Sébastien Ciukaj (1)

(1) CTMNC, 200 avenue du Général-de-Gaulle, F-92140 Clamart Cedex
(2) Laboratoire PHASE, 118 route de Narbonne, Université Toulouse 3, F-31062 Toulouse Cedex
(3) CSTB, 24 rue Joseph Fourier, F-38400 Grenoble Cedex

PACS: 43.40.Rj

ABSTRACT

The modelling of sound transmission loss (STL) through multi alveolar brick walls is investigated. Because of the complex structures involved, a simplified approach is derived. First, an efficient homogenization technique is developped to define an equivalent orthotropic block. Then, the STL of the homogenized wall is computed thanks to a finite and multi-layered anisotropic thick plate model. A modal analysis is also performed on various hollow brick walls to confirm the predictions of the model. Finally, a parametric study highlights the relevant physical parameters for the improvement of the acoustic properties of those materials.

INTRODUCTION

Because of their thermal properties, hollow bricks are attractive building elements. Typical core geometries of hollow blocks are depicted in Figure 1.

Figure 1. Different hole pattern of fired clay blocks

Unfortunately, the acoustic behaviour of such walls is complex since it strongly differs from others homogeneous building elements. This point is clearly observed in Figure 2 where the well known mass law [1] is compared to the STL measured for two hollow brick walls. Various dips and peaks can be seen in the measured curves due to the complex properties of these walls (inhomogeneous, anisotropic, thick). The aim of this work is to understand the physical behaviour of brick walls.
From a numerical point of view, the simulation of the STL of a hollow brick wall is possible [2] but complex blocks may require very long computation times. Besides, analytical developments on the STL through periodically inhomogeneous plates [3-4] are also too time consuming if one has to treat with a realistic situation (typically a masonry wall).

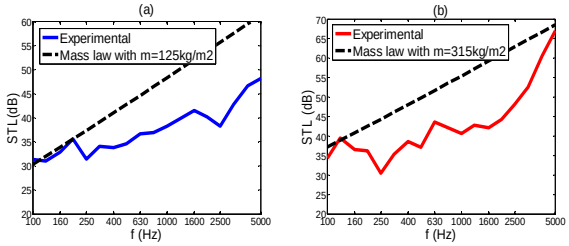

Figure 2. STL measured on a (a): 20cm thick hollow brick (b): 30cm thick wall. In both cases, results are compared with $STL_{mass} \approx 20\log\left(\frac{\pi mf}{\rho_{air}c_{air}}\right)$ where $\rho_{air}c_{air}$ is the air impedance and m the mass density of the wall

Therefore, in this paper, a simplified modelling is adopted. In first approximation, the inhomogeneous brick can be replaced by an equivalent homogeneous one using homogenization theories [5-6]. This approximation is relevant provided that the size of the inhomogeneities is small compared to half the wavelength of the vibrations [3]. Since the size of the holes in a hollow brick does not exceed few centimeters, an homogenized vibratory model should be a reliable solution in the frequency range [100Hz-5kHz].

AN HYBRID MODEL TO COMPUTE THE STL OF A HOLLOW BRICK WALL

STL of an orthotropic thick plate

Considering homogenization theories mentionned above, one is lead back to the STL of an equivalent multi-layered anisotropic masonry wall. The transfer matrix formalism

derived by Skelton & al. [7] is used to solve that problem. Then the transmission coefficient of the wall is given by

$$\tau^{\text{diffuse}} = \frac{1}{\pi}\iint_{\theta,\varphi}\tau(\theta,\varphi,f)\sin(\theta)\cos(\theta)\,d\theta\,d\varphi$$
$$\tau(f,\theta,\varphi) = |T|^2, T = \frac{2ZL_{21}}{L_{12}L_{21} - (L_{11}+Z)(L_{22}-Z)}, Z = \frac{\rho_a c_a}{\cos(\theta)} \quad (4)$$
$$0 \le \varphi \le 2\pi, 0 \le \theta \le \theta_{\max}$$

Where the assumption of a diffuse incident field has been made and $L_{ij}, i,j = 1,2$ are the matrix elements connecting normal stresses and velocities of the upper and lower surfaces of the wall.
Under this form, the finite dimensions of the wall are not taken into account. A more suitable solution is

$$\tau_{\text{finite}}(f,\theta,\varphi,L_x,L_y) = \tau_\infty(f,\theta,\varphi)\sigma(f,\theta,\varphi,L_x,L_y) \quad (5)$$

Where a correction function σ is introduced according to the spatial filtering technique [8]. This approach takes into account the diffraction effect induced by the finite size of the wall. However, no modal behaviour can be recovered in this manner since the boundaries conditions are not considered.
Therefore, the STL of the homogenized brick wall can be explicitly written as

$$STL(f) = -10\log\left(\tau_{\text{finite}}^{\text{diffuse}}\right) \quad (6)$$

Obviously, this formalism needs the knowledge of the physical properties of the equivalent wall (elastic tensor, mass density). That is the reason why an efficient homogenization technique is developped in the following section.

A numerical homogenization process

The basic principle is to simulate different mechanical loadings applied to one block. To this end, an orthotropic model is adopted and a finite element method (FEM) expansion is used.
When subjected to a compression test along the i axis (i=x,y,z), the Young modulus along that direction and the Poisson ratios associated with the corresponding planes are

$$\begin{cases} E_i = -\dfrac{F_i L_i}{L_j L_k}; j,k = x,y,z; k \ne j \\ \upsilon_{ij} = -\dfrac{u_j L_i}{L_j}; i \ne j \end{cases} \quad (7)$$

Where $F_i, L_{i,j,k}, u_j$ are respectively the force reaction on the face $i = L_i$, the hollow block dimensions and the displacement induced by the Poisson effect.
Consequently, six of the nine elastic constants are obtained with compression tests. To compute the last three shear modulus, adapted boundaries conditions are deduced from pure shear stresses. The different computed loads are summarized in Figure 3. Then, the shear modulus is evaluated by

$$G_{ij} = \frac{T_{ij}}{\gamma_{ij}} = \frac{T_{ij}}{2}; i,j = x,y,z; i \ne j \quad (8)$$

With T_{ij} the shear stress in the plane ij and γ_{ij} the distorsion angle induced by the shearing.

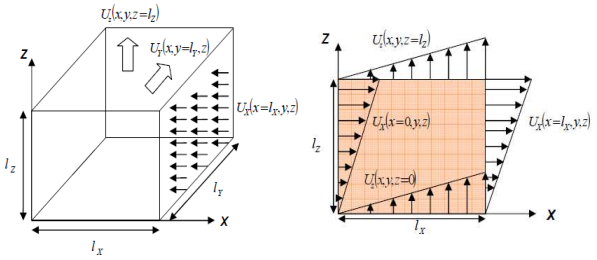

Figure 3. Examples of two numerical tests : Compression along the X axis and Shear loadings in the XZ plane

Finally, the homogenized brick is characterized by the following elastic tensor

$$\overline{\overline{C}} = \begin{pmatrix} C_{11} & C_{12} & C_{13} & 0 & 0 & 0 \\ C_{12} & C_{22} & C_{23} & 0 & 0 & 0 \\ C_{13} & C_{23} & C_{33} & 0 & 0 & 0 \\ 0 & 0 & 0 & C_{44} & 0 & 0 \\ 0 & 0 & 0 & 0 & C_{55} & 0 \\ 0 & 0 & 0 & 0 & 0 & C_{66} \end{pmatrix} \quad (9)$$

Comparison between simulations and measurements

The former approach is now applied to the prediction of sound transmission through the whole masonry: The first layer is built from hollow bricks and covered by an additionnal plaster lining.
This second layer is considered as an isotropic layer whose properties are : $E = 5GPa$, $\upsilon = 0.2$ and $\rho = 1500kg/m^3$. The STL of each wall is determined using standard technique, according to the IS0 140-3 norm [9].
Besides, quantitative predictions are possible only if two experimental key parameters are known. The first one is the set of mechanical parameters for the brick material (the clay material). Their knowledge, along with that of the hollow core geometry, will obiously affects the values of the homogenized tensor $\overline{\overline{C}}$. Ultrasonic measurements have been performed to determine these elastic constants.
The second one is the damping. A practical way to include it in the model is to consider a complex elastic tensor :

$$\overline{\overline{\tilde{C}}} = \overline{\overline{C}}(1 - i\eta) \quad (10)$$

In that expression, η stands for the total loss factor of the wall and includes internal, radiation and coupling loss factors. Structural reverberation times measured on each partition give an estimation of this frequency dependent variable [10].
The first example is a 20cm thick wall covered by a 1cm thick plaster layer. The hole pattern of the brick and its homogenized parameters are given in Figure 4 and Table 1.

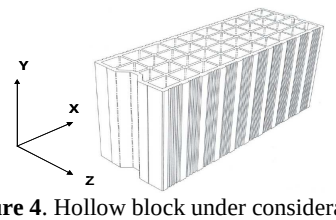

Figure 4. Hollow block under consideration
$\left(L_x = 56cm, L_y = 27cm, L_z = 20cm, \rho_{eq} \cong 595kg/m^3\right)$

The computed values are consistent with the alveolar pattern that have been tested. First, the fact that $E_X \approx E_Z$ expresses the nearly isotropic behaviour of this block in the (XZ) plane.

The high softness in that plane also explains the low value of the shear modulus $G_{XZ} = C_{55}$. On the contrary, the Young modulus along the Y direction is the highest one for two reasons. First, this direction matches that of the stiffest rididity of the brick material. Furthermore, in that direction, the stiffness of the block and the clay are directly related by $E_Y^{brick} = S_{clay}(l_X l_Z)^{-1} E_Y^{clay}$ (with $S_{clay} << l_X l_Z$ and $E_Y^{brick} << E_Y^{clay} \cong 10GPa$).

Table 1. Parameters of the equivalent orthotropic brick wall

Ex (GPa)	Ey (GPa)	Ez (GPa)	Gxy (GPa)	Gxz (GPa)	Gyz (GPa)	υ_{yz}	υ_{xy}	υ_{zx}	$\rho_s(kg/m^2)$
0.48	2.18	0.44	0.3	0.22	0.42	0.19	0.12	0.01	125

Figure 5 shows the experimental STL and the calculated one. The orthotropic thin plate approximation, which can be found in ref [11], is also computed. In low frequencies, the experimental dip is well predicted and corresponds to the usual critical region of thin anisotropic plates. For an orthotropic plate, this region is bounded by the two critical frequencies

$$f_{cx} = \frac{c_a^2}{2\pi}\sqrt{\frac{\rho_s}{B_x}} \text{ and } f_{cy} = \frac{c_a^2}{2\pi}\sqrt{\frac{\rho_s}{B_y}} \quad (11)$$

Where B_x and B_y are the bending stiffness of the homogenized wall along the x and y axis.

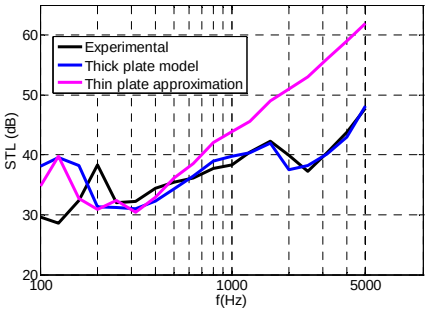

Figure 5. Comparison between simulations and test data

Above [700Hz-800Hz], the thin plate approximation is clearly no longer valid for this wall. Measurement shows another dip higher in frequency, around 2.5kHz. This decrease of the STL is predicted only by the thick plate model. Unlike the thin plate assumption, this model considers the radiation of all Lamb modes existing in the homogenized wall. Because of its spatial shape, the first symmetric Lamb mode S1 may radiate from its cut off frequency

$$f_{S1} \cong \frac{1}{2}\sqrt{\frac{E_z}{h\rho_s}} \quad (12)$$

For the studied wall, numerical calculation localizes this frequency around 2200Hz, namely in the range where the STL drops.

The second example is devoted to the study of a 37.5cm thick brick wall (covered by a 1.5cm thick plaster layer). Compared to the first 20cm thick wall , both thickness and core geometry are designed to minimize heat transmission (see Figure 6).

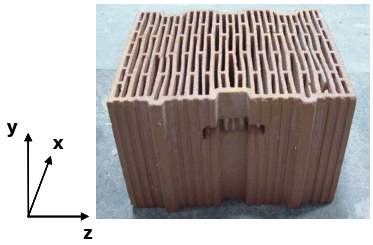

Figure 6. Schematic view of the thick hollow block $\left(L_x = 27.5cm, L_y = 21cm, L_z = 37.5cm, \rho_{eq} \cong 940kg/m^3\right)$

Homogenized parameters for this hollow structure are summarized in Table 2 and call for several comments. In the y direction, the Young modulus is the highest one for the same reason as before. In the same way, the core geometry in the xz plane is consistent with a very low shear modulus $G_{XZ} = C_{55}$. A great attention should be also paid to the very high softness of the block along the thickness direction. This point is directly due to the thermal constrain which often lead to winding profiles.

Table 2. Homogenized parameters

Ex (GPa)	Ey (GPa)	Ez (GPa)	Gxy (GPa)	Gxz (GPa)	Gyz (GPa)	υ_{yz}	υ_{xy}	υ_{zx}	$\rho_s(kg/m^2)$
2.1	6.76	0.13	0.82	0.07	0.63	0.18	0.17	0.01	400

Figure 7 displays the STL predicted by the complete hybrid model along with the approximate one with the measurement. The critical region is located in very low frequencies (roughly between 60Hz and 100Hz).
Such hollow brick wall cannot be seen as a thin homogenized plate over most of the frequency range of interest (except in low frequencies). A large wall thickness coupled with a very high softness of the wall along the z direction are responsible for this thick plate behaviour. In other words, the drop of the STL around 500Hz is caused by the S1 Lamb mode radiation (numerical calculation gives $f_{S1} \cong 460Hz$).

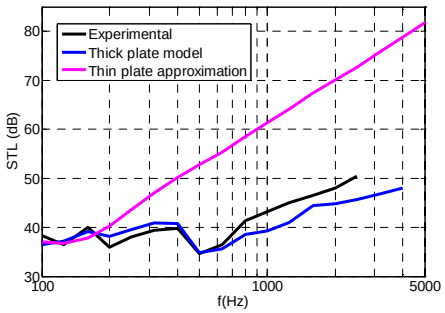

Figure 7. Results obtained on a 39cm thick brick wall

The main predictions made in this part will be verified in the following section.

MODAL ANALYSIS

Lamb modes in homogeneous plates have been extensively studied [12,13]. Though, in a building acoustic context, the vibratory behaviour of complex walls such as hollow brick ones remains an open question. To confirm the existence of Lamb modes like in these partitions, an experimental and numerical modal analysis are performed.

Experimental study

From an experimental point of view, a masonry wall of dimensions $2.98\times3.78\times0.2\text{m}^3$ made of the former hollow blocks (see Figure 4) has been built. One brick of that wall is mechanically excited using a shaker that generates a white noise signal in the range [100Hz-5kHz].
The vibratory response of the wall is then investigated with various pairs of accelerometers. A scheme of the experimental setup is given in Figure 8.

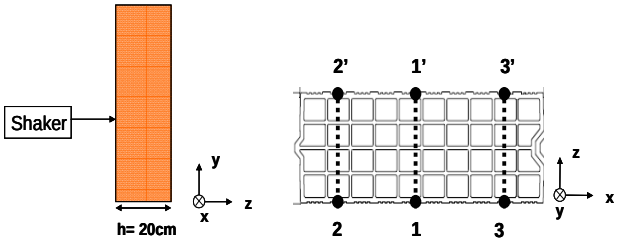

Figure 8. Schematic view of the experience. For each pair of accelerometers (k,k') (with $k,k'=1,2,3$), the accelerometers k and k' are located at $(x_k, y_k, z_k=0)$ and $(x_k, y_k, z_{k'}=21\text{cm})$

In our experiment, the frequency dependence of the relative phase between each accelerometer k and k' may give precious information on the spatial shape of the vibrating wall.
Therefore, the phase of the following transfer function H is measured

$$\Delta\theta_{k,k'}(f)=\arctan(H)=\arctan\left\{10\log\left(\frac{v_z^{k'}}{v_z^{k}}\right)\right\}=\theta_{k'}-\theta_k \qquad (13)$$

Where v_z^k, $v_z^{k'}$ are the normal velocities measured by the accelerometer k and k' (respectively). Results are reported on Figure 9.

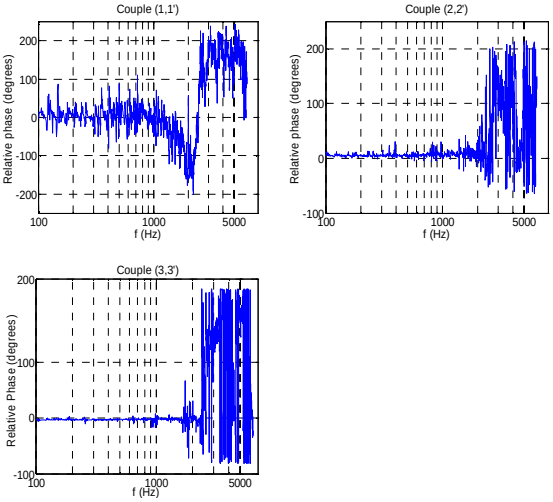

Figure 9. Phase shift measured on the different couples of sensors

Two behaviours are highlighted. From 100Hz to approximately 2000Hz , the phase shift between the two sides of the brick wall are (in average) equal to zero. This is consistent with the hypothesis of bending waves propagating in the partition.
Around the cut off frequency of the S1 Lamb mode of this homogenized wall (see equation 12), each couple of accelerometers are in opposite phase. Thus the vibration of the inner and outer surfaces of the wall are out of phase from this frequency.

Numerical modelling of the vibratory behaviour

To complete this experimental study, two hollow block walls (see Figures 4 and 6) are now simulated thanks to a 2D finite element model. As before, a constant force F is applied and the vibratory responses of the walls are recorded on different pairs of nodes. Figure 10 summarizes the numerical experience.

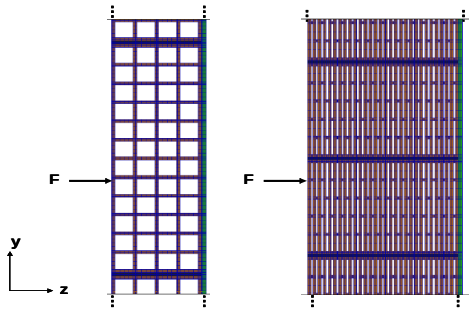

Figure 10. Close-up on the $2.84\times0.21\text{m}^2$ (left part) and $2.27\times0.39\text{m}^2$ (right part) simulated walls. In both cases, the plaster layer (in green) and the small bed joints (in black) between blocks are also represented

The relative phase between the inner and outer surfaces of both walls is reported on Figure 11. Those results are in good agreement with both the predictions made above and the experimental modal analysis. In each case, this phase shift equals zero until the cut off frequency of the S1 Lamb mode of the homogenized wall. From this frequency, the phase shift signal exhibits oscillations with (in average) a 180° out of phase. Some spatial deformed of the brick walls for different frequencies are also shown.

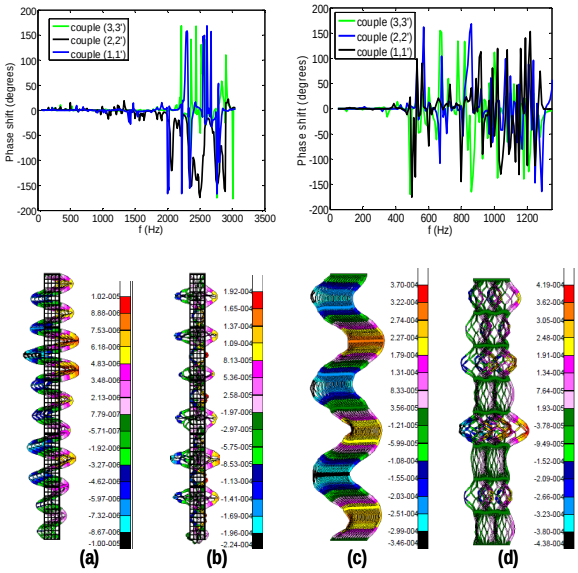

Figure 11. FEM computation of the phase shift for the 21cm thick wall (left upper part) and the 39cm thick one (right upper part). (a) & (b): Visualization of the normal velocities Vz(y,z) at 700Hz and 2500Hz (respectively); (c) & (d): Visualization of the normal velocities Vz(y,z) at 350Hz and 620Hz (respectively)

A PARAMETRIC SURVEY

This last part presents some hints to impove the STL of hollow block walls. In practice, two parameters of the wall can be modified: the geometry of the block and the brick

material itself. This one is kept constant here and our attention is focused on the hollow geometry.

General considerations

Many input parameters are needed to compute the STL of the wall : thickness, mass density and elastic tensor of the homogenized brick. It is logical to first analyze the relative impact of each parameters. Considering a 20cm thick hollow brick whose homogenized parameters are given in Table 3, each component of its elastic tensor is submitted to a 50% variation. Note that the Poisson ratios do not appear because their impact on the STL is negligible

Table 3. Homogenized constants of the block

Ex (GPa)	Ey (GPa)	Ez (GPa)	Gxy (GPa)	Gxz (GPa)	Gyz (GPa)	ρ_{eq} (kg/m^3)
0.63	2.9	0.57	0.52	0.26	0.69	547

The results of this parametric study are reported on Figure 12. In low frequencies, the main impact comes from Ex, Ey and Gxy because these parameters are “thin plate constants”.
If the Young modulus Ex and Ey are modified, the critical region is also changed [10]. From this point of view, the more anisotropic the plate is, the wider the critical region and the more badly affected the STL is.
Higher in frequencies, those parameters do not play a significant purpose anymore. On the contrary, a change in the rigidity in the thickness direction is seen to produce an important increase of the STL. This is due to the resonance of the S1 Lamb mode (see equation 9). Besides, the shear modulus Gxz and Gyz are also important to improve the acoustic behaviour of hollow block walls.

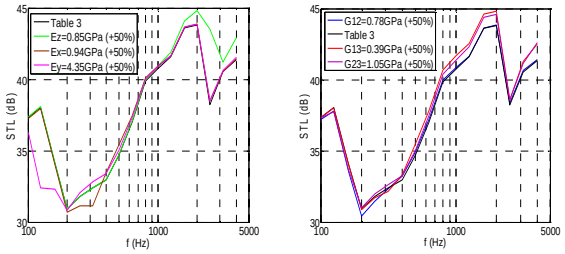

Figure 12. Influence of the Young modulus (left part) and the Shear modulus (right part) on the STL

Using those general considerations, the inverse problem is now adressed. In other words, the hollow core geometry itself is modified in order to optimize its homogenized constants.

Application to various hollow core patterns

Three cases are considered: the first one is a hollow geometry where the holes describe a simple square lattice. The second one is the same block where the thickness rigidity is enhanced thanks to a higher number of connecting bridges. The last studied geometry is deduced from the previous one by additionnal connections in the brick interior.
These cases and their homogenized parameters are resumed in Figure 13 and Table 4.

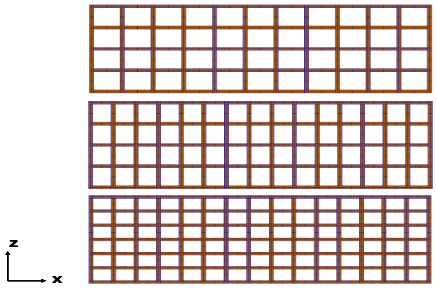

Figure 13. Various hollow cores considered: square lattice (upper), rectangular lattice (middle) and square lattice with smaller holes

Table 4. Equivalent constants of the different hollow bricks

	Ex (GPa)	Ey (GPa)	Ez (GPa)	Gxy (GPa)	Gxz (GPa)	Gyz (GPa)	ρ_{eq} (kg/m^3)
Case 1	0.97	1.52	0.89	0.38	0.26	0.45	547
Case 2	0.99	1.73	1.17	0.31	0.1	0.46	624
Case 3	1.37	2	1.2	0.29	0.12	0.47	724

The STL associated with these cases are shown in Figure 14. If one considers first the influence of the mass density, two points should be mentionned. According to the mass low, the STL is the best one in the last case (namely the heavier one) in very low frequencies.
However, this figure demonstrates the possibility to conceive light but efficient hollow brick walls. In particular, thanks to its equivalent mechanical parameters, the first case presents the best STL in a very large frequency range.
This is mainly due to the sensibility of the shear modulus Gxz to the modification of the hole pattern. In the second case, the Young modulus Ez increases but a strong decrease of the shear modulus Gxz is also associated (compared to the first one). This decrease results from the rectangular pattern of the holes in the second case.
Therefore, in the last case, a square pattern is reconstructed but only a small increase of Gxz is obtained (compared to the second case) because now the holes have small square sections.

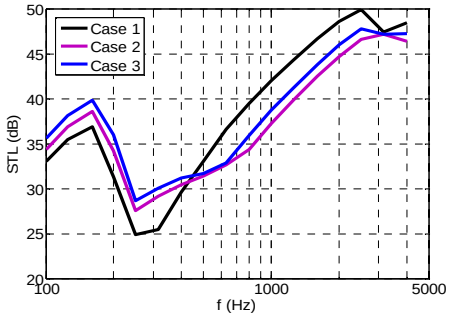

Figure 14. Influence of the core geometry on the STL predicted

This parametric study is finally applied to hollow blocks of common use in practice (20cm thick). As mentionned above, the hole pattern is mainly designed to improve the thermal insulation of the wall.
Here again, three cases are treated: the first one (labelled “reference case”) has a simple square lattice of holes. The second one is modified in order to lower thermal bridges. In the same way, the last block is conceived to minimize heat transmission (see Figure 15). Table 5 reports the

homogenized parameters in each situation while the various predicted STL are given in Figure 16.

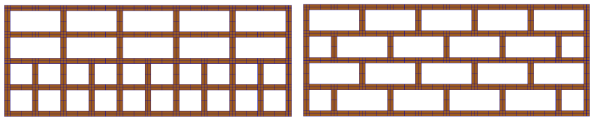

Figure 15. Picture of the "thermal" hollow blocks. The brick labelled "thermal block 1" is on the left while the "thermal block 2" is on the right.

Because of the very low stiffness of the "thermal block 2" along the thickness direction, the computed STL exhibits a huge decrease between 1500Hz and 2500Hz due to the resonance of the S1 Lamb mode. An intermediate solution is provided by the "thermal brick 1" where the acoustical loss seems less critical.

Table 5. Homogenized parameters of the different bricks

	Ex (GPa)	Ey (GPa)	Ez (GPa)	Gxy (GPa)	Gxz (GPa)	Gyz (GPa)	ρ_{eq} (kg/m^3)
Reference case	1.39	2	1.29	0.56	0.39	0.64	751
Thermal Brick 1	1.36	1.9	0.78	0.55	0.37	0.63	684
Thermal Brick 2	1.33	1.75	0.3	0.54	0.37	0.44	629

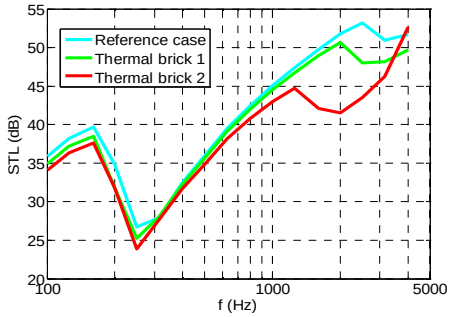

Figure 16. Impact of the thermal constrain on the predicted STL

CONCLUSION

The acoustic behaviour of masonry walls made of hollow bricks is studied. First of all, the brick wall is considered as a thick orthotropic plate. An efficient technique, based on homogenization theories, is derived to obtain the properties of the homogenized brick. The vibratory behaviour of different brick walls is analysed and compared to the STL predicted. As expected, such walls display usual features of thin anisotropic plates in low frequencies. However, their large thickness and low stiffness in the thickness direction are responsible for additionnal resonances where the wall exhibit symmetric vibrations (due to the S1 Lamb mode). The model is then used to quantify the impact of each equivalent parameters and applied to underline the STL properties of various hollow blocks.

REFERENCES

1 F. Fahy, *Sound and structural vibration* (Academic Press, second edition, 2007)

2 P. Jean and M. Villot, "Finite element modelling of sound transmission through heavy heterogeneous masonry" *Proceedings of EURONOISE* (1987)

3 J. Wang, T.J Lu, J. Woodhouse, R.S Langley, J. Evans "Sound transmission through lightweight double-leaf partitions: theoretical modelling" *Journal of Sound and Vibration*. **286**, 817–847 (2004)

4 W. Maysenholder and R. Haberkern, "Sound transmission through periodically inhomogeneous plates: solution of the general problem by a variationnal formulation" *Acta acustica*. **89**, 323–332 (2003)

5 W. Maysenholder, "Low frequency transmission through periodically inhomogeneous plates with arbitrary local anisotropy and arbitrary global symmetry" *Acta acustica*. **82**, 628–635 (1996)

6 E. Sanchez-Palencia and A. Zaoui, *Homogenization techniques for composite media* (Springer, 1985)

7 E.A. Skelton and J.H James, "Acoustics of anisotropic planar layered media" *Journal of Sound and Vibration*. **152**, 157–174 (1992)

8 M. Villot, C. Guigou and L. Gagliardini, "Predicting the acoustical radiation of finite size multi-layered structures by applying spatial windowing on infinite structures" *Journal of Sound and Vibration*. **245**, 433–455 (2001)

9 ISO 140-3:1995 (E) "Acoustics: Measurements of sound insulation in buildings and of building elements". *International Organization for Standardization, Genève, Switzerland*.

10 V. Hongisto, M. Lindgren, R. Helenius "Sound insulation of double walls – An experimental parametric study" *Acta acustica*. **88**, 904–923 (2002)

11 A. Ordubadi an R.H. Lyon "Effect of orthotropy on the sound transmission through plywoods panels" *Journal of the Acoustical Society of America*. **65**, (1979)

12 H. Lamb "On waves in an elastic plate" *Conf. of the royal society*. **88**, (1917)

13 D. Royer and E. Dieulesaint *Elastic waves in solids* (Masson, 2000)